

Skeletal development and adult osteology of *Hypsiboas pulchellus* (Anura: Hylidae)

JULIO M. HOYOS¹, MARCELO R. SÁNCHEZ-VILLAGRA², ALFREDO A. CARLINI³, CHRISTIAN MITGUTSCH^{2*}

¹ Pontificia Universidad Javeriana, Facultad de Ciencias, Departamento de Biología, Unidad de Ecología y Sistemática, A.A 56710, Bogotá, D.C., Colombia.

² Paläontologisches Institut und Museum, Universität Zürich, Karl Schmid-Strasse 4, CH-8006 Zürich, Switzerland. *Corresponding author. E-mail: christian.mitgutsch@gmail.com

³ Paleontología de Vertebrados, Museo de La Plata, Paseo del Bosque s/n (B1900FWA), La Plata, Buenos Aires, Argentina.

Submitted on:

Abstract. Osteological and skeletal characters have long been proven to be particularly informative in taxonomic and systematic research. Furthermore, ossification sequences are assumed to be a potential tool to investigate developmental states and developmental modes of fossil and extant skeletal specimens. Herein, we provide a detailed account on adult osteology and skeletogenesis in the Montevideo treefrog, *Hypsiboas pulchellus* (Anura: Hylidae) based on evaluation of a series of cleared and stained specimens. A consensus sequence of ossification, i.e., the order of appearance of mineralized elements until early metamorphosis could be determined as (parasphenoid, presacral vertebrae I-VII, frontoparietal, exoccipital) – transverse processes of presacral vertebrae I-VIII – sacral vertebra – (humerus, radioulna, ilium, femur, tibiofibula, scapula) – (cleithrum, clavicle, coracoids, metacarpals, tarsals, metatarsals, phalanges, hypochord) – (prootic, angulosphenial, dentary, maxilla, premaxilla, squamosal). Comparing the state of mineralized elements in individual specimens, a number of skeletal elements, including the exoccipital, frontoparietal, parasphenoid and prootic, as well as elements of the shoulder and pelvic girdles, and the phalanges, were found to vary intraspecifically regarding the relative time of their ossification within the ossification sequence.

Keywords. Anuran anatomy, comparative developmental biology, Hylidae, *Hypsiboas pulchellus*, sequence of ossification, skeletogenesis

INTRODUCTION

Studies of osteology and skeletal development in anuran amphibians have a long legacy in biological research; the relative ease of access to embryos and a stunning diversity of

life histories render anurans to be particularly suitable targets for comparative studies in skeletal and skeletogenic evolution. In particular, understanding the evolution of skeletal repatterning in metamorphosing species is a subject worth of investigation (e.g., Duellman and Trueb, 1994; Gurdon and Hopwood, 2000; Callery, 2006; Crump, 2009).

Detailed descriptions of anuran skeletons are available from a wide range of taxa, both extinct and extant. Summaries of osteological patterns and interpretations of taxonomic distributions of osteological characters can be found in Trueb (1973, 1993), Báez (2000), Rage and Roček (2000), Roček (2000, 2003), Clarke (2007); examples of in-depth descriptions and discussions of anuran chondrocrania in Gaupp (1896), Ramaswami (1944), van Eeden (1951), de Sá and Trueb (1991), Haas (1995), de Sá and Hill (1998), Larson and de Sá (1998), Swart and de Sá (1999), Larson (2002), and Larson et al. (2003). Particularly, the cranial development of frogs has been discussed in connection with a variety of topics, including conceptual issues such as head segmentation (Vogt, 1842; Stöhr, 1881) and life history evolution including traits and topics such as direct development, metamorphosis, or miniaturization (e.g., Trueb and Alberch, 1985; Hanken et al., 1992; Rose and Reiss, 1993; Yeh, 2002; Maglia et al., 2007; Kerney et al., 2007, 2010).

In the context of vertebrate skeletogenesis, special focus has been given to the evolution of ossification sequences, i.e., accounts on the relative order in which bones ossify in a given taxon. Heterochronies within ossification sequences have been shown to be potentially informative about life history traits (Weisbecker et al., 2008). Furthermore, ossification sequences could enlighten the life histories of fossil embryonic specimens using an extant phylogenetic bracket (e.g., Balanoff and Rowe, 2007). Great effort has been put into establishing ossification sequences in a considerable variety of species from a wide range of vertebrate taxa. Tools to analyze ossification sequences and temporal sequences of other developmental events have been developed and applied in a variety of studies (e.g., Nunn and Smith 1998; Richardson et al., 2001; Jeffery et al. 2002a, b, 2005; Koenemann and Schram, 2002; Poe and Wake, 2004; Schulmeister and Wheeler, 2004; Harrison and Larsson, 2008; Germain and Laurin, 2009). From several taxa however, increasing evidence has been accumulated that intraspecific variation in ossification sequences might be considerable and that ossification sequences potentially evolve relatively quickly (Hanken and Hall, 1984; Dunlap and Sanchiz, 1996; Mabee and Trendler, 1996; Mabee et al., 2000; Bininda-Emonds et al., 2003; Moore and Townsend, Jr., 2003; Sheil and Greenbaum, 2005; Maxwell, 2008; Weisbecker and Mitgutsch, 2010; Mitgutsch et al., 2011). As a consequence, while ossification data are available from a broad taxonomic range, the scarce availability of taxonomically densely sampled datasets makes closer investigations of such sets highly desirable.

De Sá and Trueb (1991) stated that for no more than 0.6% of all described anuran species ossification sequences have been reported. Since then, several ossification sequences for neobatrachians in general and for hylids in particular have been published, but also many more new anuran species have been described. Sheil and Alamillo (2005) emphasized that very few osteological or developmental descriptions of hylids exist, given the total number of hylid species described (almost 900). Besides, some of the studies in which ossification sequences were reported, do not provide information on postcranial ossification although a number of studies did cover descriptions of whole ossification sequence (De Sá, 1988; Haas, 1996; Maglia and Púgener, 1998; Púgener and Maglia, 1997; Dunlap and Sanchiz, 1996; Wiens 1989; Haas, 1999; Wild, 1999; Sheil and Alamillo 2005;

Trueb et al., 2000). Within hylids, either cranial or postcranial ossification sequences are available for a number of species, namely *Hypsiboas lanciformis* (de Sá 1988), *Pseudacris triseriata* (Stokely and List 1954), *P. regilla* (Gaudin 1973), *Phyllomedusa vaillanti* (Sheil and Alamillo 2005) *Smilisca baudinii*, *Tripurion petasatus*, and *Osteopilus septentrionalis* (Trueb 1970); for a summarized comparison of the cranial ossification patterns in these species see Weisbecker and Mitgutsch (2010).

In the present study, we describe the development and the adult osteology of both the cranial and postcranial skeleton of a hylid frog species, the Montevideo treefrog, *Hypsiboas pulchellus*. Furthermore, we provide information about intraspecific variation in the relative order of the onset of ossification in individual skeletal elements.

MATERIALS AND METHODS

Specimens of *Hypsiboas pulchellus* (Duméril and Bibron, 1841) were collected from the wild near La Plata, Argentina. The animals were anesthetized and fixed in 4% buffered formaldehyde. After fixation, the frogs were cleared and double stained for the visualization of mineralized bone and cartilage with alcian blue and alizarin red following standard laboratory protocols (Dingerkus and Uhler, 1977). Prior to documentation, selected specimens were partially dissected to allow for visualization of individual parts of their skeletons.

To study intraspecific variation in ossification orders, ontogenetic states-tables were filed as suggested by Mitgutsch et al. (2011). The numbers of specimens sharing one ontogenetic state are shown in Fig. 8. Skeletal specimens examined were: one adult male specimen, one freshly metamorphosed froglet and 32 tadpoles of Gosner-stages (GS; Gosner, 1960) GS43/44 (2 individuals), GS42 (3), GS41 (5), GS39/40 (4), GS 37 (1), GS36 (3), GS35 (2), GS34 (3), GS33 (2), GS31 (2), and GS30 and younger (5).

Anatomical nomenclature herein is largely on the basis of Haas (1999) and Sheil and Alamillo (2005); for further discussions see Trueb (1973) and Roček (2003).

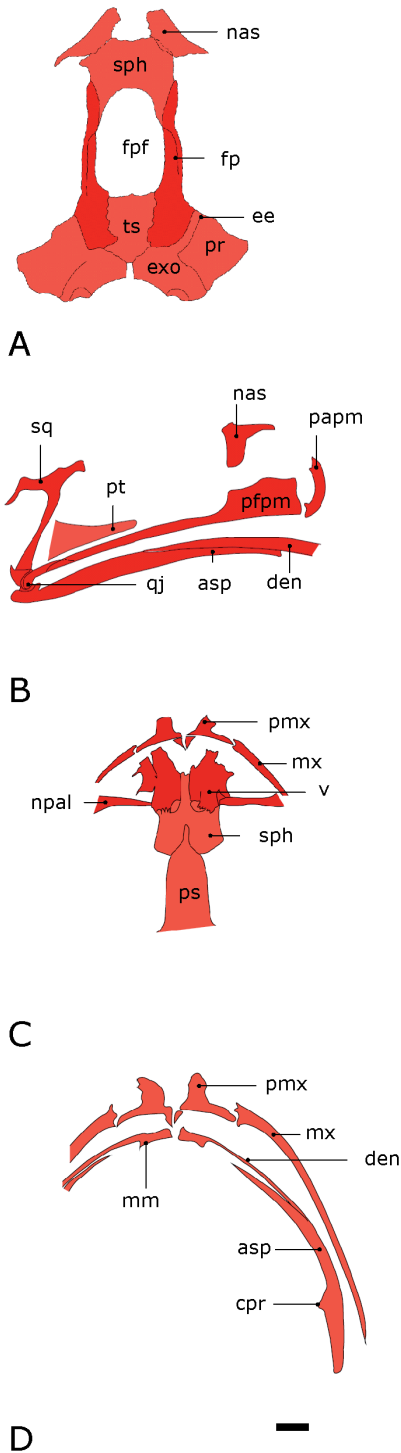
RESULTS

Adult osteology

Cranium (Fig. 1A-D)

The septomaxillae are paired bones located dorsally to the vomers, within the nasal capsules and embedded in the nasal cartilages. They are situated posterolateral to the alary cartilages. Each septomaxilla has three processes: anterolateral, dorsomedial and posterior. The dorsomedial and the posterior processes are longer than the anterolateral process. The septomaxillae are medially separated.

The nasals are paired bones, have a crescent shape, lying in an oblique position. They are separated medially; the septum nasi is not covered by them. The posterior margin of each nasal invests (or overlaps) the anterior margin of the sphenethmoid. The maxillar process is large, articulating with the pars facialis of the maxilla. They do not have a rostral process; they are not in contact with the premaxilla.



The frontoparietals are paired and narrow bones separated by a large gap. Their medial borders are concave, the lateral borders convex. The anterior ends overlap with the dorsolateral and the posterior edge of the sphenethmoid. Posterolaterally, each bone invests both the epiotic eminence (= eminentia epiotica) of the prootic and the anterior end of the exoccipital bone.

The parasphenoid is a flat, in ventral view T-shaped appearing bone, the long bar pointing anteriorly. The cultriform process is pointed at the anterior end, wide in the middle and constricted posteriorly. The parasphenoid alae are distally truncated, slightly inclined, extending posterolaterally to invest the lateral border of the otic capsules (prootic and exoccipital). The posteromedial process reaches the ventral margin of the foramen magnum.

The vomers are paired and dentigerous (six teeth). They are medially articulated to each other and are posteriorly either articulated or fused to the proximal end of the palatine bones; the vomers are not articulated to the pars facialis of the maxilla. The vomers have four processes: the odontophore (dentigerous process) is slightly inclined and posterior to the palatine. The pre- and postchoanal processes are very short, placed anterior and posterior to the odontophorous process. The vomers have a free and truncated anterior process. Posteriorly, the vomers are fused to the anterior border of the sphenethmoid.

The premaxillae are upside down T-shaped, paired bones consisting of three parts: pars alaris, p. palatina, and p. dentalis. The pars alaris projects posterodorsally; the dorsal ends of the partes alares have a notch. The pars dentalis is the base of the

Figure 1. Skeletal elements of the adult cranium. A) Dorsal, B) lateral, C) dorsal view; D) ventral view on jaw and maxilla. Abbreviations: asp, angulosphenial; cpr, coronoid process; den, dentary; ee, epiotic eminence; exo, exoccipital; fp, frontoparietal; fpf, frontoparietal fenestrum; mm, mentomeckelian; mx, maxilla; nas, nasal; npal, neopalatine; papm, pars alaris premaxillaris; pfp, pars facialis premaxillaris; pmx, premaxilla; pr, prootic; ps, parasphenoid; pt, pterygoid; qj, quadratojugal; sph, sphenethmoid; sq, squamosal; ts, tectum synoticum; v, vomer. Scale 1 mm.

“T” bearing the teeth. The partes dentales are separated by a narrow space between them. In our largest specimen we found 15 teeth in each of the partes dentales. The posterolateral element of the pars dentalis (or pars facialis sensu Sheil et al. 2005) slightly overlaps with the anterolateral end of the pars facialis of the maxilla. Each pars palatina bears triangular, prominent posteromedial processes, slightly widened posterolaterally. These processes contribute to the articulation of the premaxillae along the medial borders of its posteromedial process. The pars palatina is as long as the pars dentalis. The posterior (distal) end is in contact with the pars palatina of the maxilla and is slightly widened. The medial part is concave, the proximal ones triangular. The premaxillar pars palatina is not articulated to the pars palatina of the maxilla.

The maxillae are composed of three parts: facialis, palatina, and dentalis. The pars dentalis of each maxilla bears nearly 60 teeth in our largest specimen. The anterior end of the pars dentalis overlaps the posterior end of the pars dentalis of the premaxilla. The maxilla extends posteriorly, overlapping laterally the first third of the quadratojugal. The pars facialis is much higher than the pars dentalis in the preorbital region, diminishing in height towards the orbital region. The pars facialis projects onto the planum antorbitale and articulates with the maxillary processes of the nasals. The pars palatina does not articulate with the pars palatina of the premaxilla.

Suspensorium

The squamosals are well ossified and triradiate: the pars zygomatica has a mediolaterally flat anterior end; pars otica has an otic plate, and the ventral (pterygoid) ramus that invests in both the external part of the quadratojugal and the distal end of the posterior arm of the pterygoid bone. The pars pterygoidea supports the tympanic annulus, and its proximal end is wider than the distal end. The posterior border of the proximal end is concave, while the distal end is flat; its maxillar slope is about 45°. The pars otica is short and wide and unornamented, bearing an otic plate which overlaps the crista parotica. The zygomatic ramus is twice as long as the otic ramus, without including the otic plate.

The pterygoid is well ossified and edentate. It has three rami arranged in a Y-shape: the anterior ramus articulates to the dorsal surface of the pars palatine of the maxilla at the level of the orbit, and just to the proximal end of the maxilla. The medial ramus articulates with the ventrolateral margin of the prootic-exoccipital. The posterior ramus invests the point of articulation of the ventral arm of the squamosal, the quadratojugal and the articular process of the angulosplenic. This ramus runs parallel and very close to the ventral ramus of the squamosal.

The quadratojugals are short bones that are positioned posterior to the maxillae. The anterior portion of the quadratojugal invests the posterior and external surface of the maxilla; it articulates with the *pars* articularis of the angulosplenic and with the inner surface of the distal end of the pterygoid branch ventral to the squamosal. The anterior and dorsal end is dagger-shaped, whereas the posteroventral end forms a cup-like base. The articular region of the palatoquadrate is ossified forming the quadrate bone and fused to the quadratojugal.

The mandibles are comprised of the mentomeckelian, dentary, and angulosplenic bones. They are well ossified and edentate. The mentomeckelian bones are located in the anterior part of the mandible and separated from their antimere by a symphyseal space.

They are fused to the dentaries. Each dentary invests laterally and externally more than one half of both the angulosplenic bone and the Meckel's cartilage. It forms the anterior half of the mandibular arch (half the length of the mandible) with a pointed posterior end. The angulosplenials extend from the posterior end of the dentaries, to its articulation with the quadratojugal by the articular process. In the prearticular region, the angulosplenic bears a medial and posterior well-developed dorsomedial coronoid process. Meckel's cartilage is found between the dentary and the angulosplenic, extending from the distal end of the mentomeckelian bones and to four-fifths the length of the angulosplenic.

The prootics and exoccipitals are fused synostotically. The exoccipitals form the posterior end of the neurocranium; they are also a part of the dorsal surface of the skull joining the frontoparietals, and most of the margin of the foramen magnum. They form the ossified and rounded exoccipital condyles too. The anterior margin of the exoccipital is part of the posterior part of the parietal fenestrum. The prootics are partially invested by the posterior end of the frontoparietals. The crista parotica is in contact with the otic plate of the squamosal; it bears posterolateral processes with cartilaginous terminal ends.

The palatines (for discussion on nomenclature see de Sá and Trueb, 1991; Trueb, 1993) are medially articulated to the vomers and to the sphenethmoid. The palatines have a distal double articulation to the maxilla: with the pars facialis and with the anterior end of the pars palatina, but do not articulate with the distal end of the anterior ramus of the pterygoid bone. It invests ventrally and posteriorly the cartilaginous planum antorbitale.

The sphenethmoid is an unpaired bone that forms the anterior part of the braincase. It is visible from dorsal between the frontoparietals and nasals, and from ventral between the vomers and the parasphenoid bone. The dorsal and posterolateral margins of the sphenethmoid are partly covered by the frontoparietals. The nasals overlap the anterior borders of the sphenethmoid. Ventrally, the sphenethmoid is a short bone extending over the anterior one third of the skull floor. Ventrally and posteriorly, the sphenethmoid reaches the anterior end of the cultriform process of the parasphenoid; the anterior border of the sphenethmoid is dorsal to the dentigerous processes of the vomers.

The annulus tympanicus of the plectral (auditory) apparatus (Fig. 2) is dorsally incomplete. The partes media et interna plectri are ossified, and fused synostotically to each other; the pars externa plectri is cartilaginous, distally enlarged, and approximately two thirds of the length of the stapes (partes interna and media plectri). The pars externa plectri has an angle of nearly 45° to the pars media plectri.

The central corpus (=hyoid plate) of the hyobranchial skeleton (Fig. 3) is partially ossified. The width of the hyoid plate is about three times the anteroposterior length. The U-shaped hyoglossal sinus is deep and wide. The cartilaginous hyalia (=hyaes sensu Maglia et al., 2007) extend posterolaterally and recurve to articulate with the otic capsule. There are no anterolateral processes. The posterolateral processes are very short compared to the posteromedial processes, with pointed posterior ends. The posteromedial processes are well ossified, with their distal and proximal ends dilated, approximately equal in width. The proximal ends are clearly separated by the posterior border of the hyoid plate. A parahyoid bone is absent. The laryngeal apparatus occupies most of the space between the posteromedial processes of the hyoid apparatus. The arytenoid cartilages are hemispherical, medially separated, with medioventral faces concave and separated. The cricoid

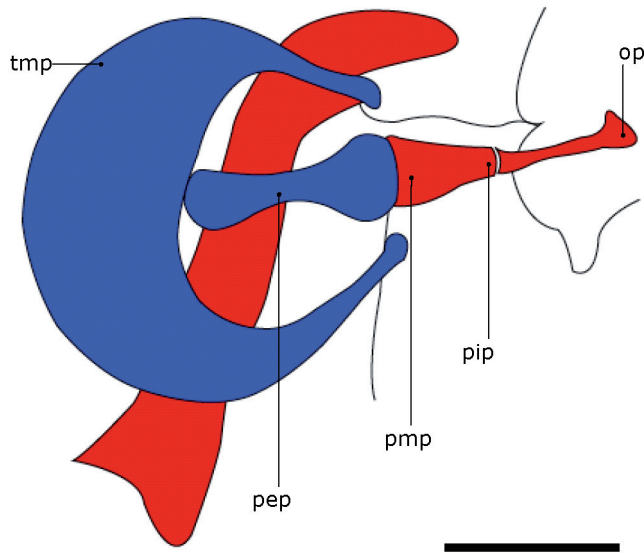


Figure 2. Auditory apparatus, abbreviations: op, operculum; pep, pars externa plectra; pip, pars interna plectra; pmp, pars media plectra; tmp, tympanic. Scale 1mm; blue: cartilage, red: mineralized bone.

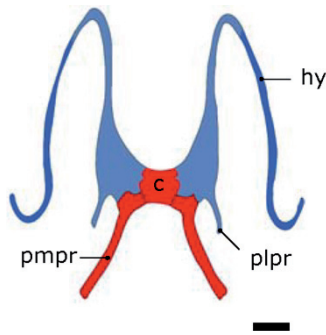


Figure 3. Hyobranchial apparatus (male). Abbreviations: c, corpus (hyoid plate); hy, hyoid; plpr, postero-lateral process; pmpr, postero-medial process. Scale 1mm; blue: cartilage, red: mineralized bone.

rings are triangular, and bear bronchial processes that extend posteroventrally from the anterolateral margins of this ring. Their distal ends are not curved medially.

Postcranium

The vertebral column comprises eight procoelous presacral vertebrae, a sacrum and the urostyle. The urostyle forms a bicondylar articulation with the sacrum. Vertebrae are not fused, neural spines are minute, and presacral vertebra VIII is not fused to the sacrum. The presacral vertebra I is type I (Lynch, 1971), having widely separated atlantal cotyles (Fig. 4). The relative lengths of the transverse processes of the presacral vertebrae are: sacral diapophyses > III > IV > VIII > II ≥ V ≥ VI ≥ VII. The transverse processes of presacral vertebrae II, VII, and VIII are oriented anteriorly, whereas those of vertebrae III, IV, and V are oriented posteriorly, and those of vertebra VI are perpendicular to the axis of the verte-

bral column. The sacral diapophyses are broadly expanded and oriented laterally from the midline of the body. The transverse processes of vertebra II are more robust than those of other vertebrae. Their lateral margins are expanded and slightly cartilaginous. The urostyle is rounded with a spinal process (urostyle crista); its sacral articulation is bicondylar. The neural spine of the axis is projected over the posterior border of the atlas.

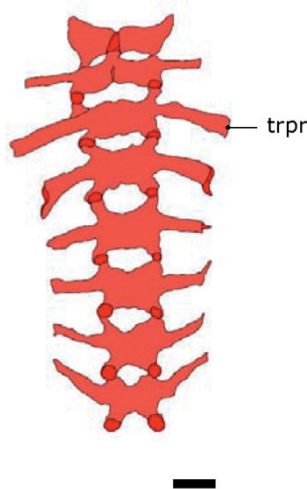


Figure 4. Adult vertebrae, dorsal view; trpr, transversal processus. Scale 1 mm.

The pectoral girdle (Fig. 5) is arciferal. The epicoracoids are ossified and broadly overlapping. The epicoracoids are connected to each other at the epicoracoid bridge, at the base of the omosternum. The procoracoid is ossified; it is continuous with the epicoracoid, bordering distally about one third of the posterior edge of the clavicles. The omosternum has two elements: the distal element, cartilaginous and expanded, and the proximal one (stylet), calcified and laterally cartilaginous. The sternum consists of one element; proximally, it is slightly calcified, distally it is cartilaginous and notched. The pectoral fenestrum is ovoid and long. The clavicles are ossified, deeply concave anteriorly and separated medially by the epicoracoid bridge. Distally close to the articulation with the pars acromialis (lateral end), they are much more expanded than at the proximal end. The clavicles are also articulated with the coracoids. The anterior and posterior margins of the coracoids are concave. The sternal (proximal) ends of the coracoids are wider than the glenoid (proximal) ends. The coracoids do not articulate with the sternum, but with the epicoracoid. The scapulae are well ossified, expanded at the ends and proximally bicapitate: their partes acromiales articulate with the clavicles, and their partes glenoidales articulate with both the coracoids and the clavicles. The scapula is nearly as long as the clavicle. The anterior margin is concave, as the proximal posterior margin, and two thirds of the distal posterior margin is convex. The distal end of the scapula articulates with the ossified suprascapula which is distally expanded and exhibits anteriorly a hooked process (processus suprascapularis, Fig. 5C). The posterior border of the suprascapula is weakly ossified. The cleithrum is well ossified, occupying nearly one third of the suprascapula. At the anterior and medial borders there is a curved process which is mostly cartilaginous but mineralized at the base.

The forelimb has proximally a well ossified humerus with a prominent crista ventralis (=deltoid crest sensu Trueb and Báez, 2006), extending over nearly the proximal two thirds of the shaft of the humerus. The proximal (glenoid) and distal (olecranon sensu Sheil and Alamillo, 2005; eminentia capita sensu Gaupp, 1896) heads are well ossified. Distally the humerus bears a short and prominent crista lateralis which extends over the distal one fourth of the anterodorsal border of the shaft of the humerus. The radioulna (for discussion of the nomenclature see Maglia and Púgener, 1998; Maglia et al., 2007) is well ossified. Although radius and ulna are fused at the midline, a distinct and incomplete sulcus intermedius (sensu Sheil and Alamillo, 2005; groove sensu Maglia and Púgener, 1998) is present. The sulcus is deeper at the distal half than at the proximal half. The radioulna is about three-fourth of the length of the humerus. It has a well-developed olecranon (=ulnar) process articulating with the distal head of the humerus. The manus (Fig. 6A) has six ossified carpal elements: ulnare, radiale, distal carpal 5-4-3, distal carpal 2, element Y and proximal prepollex. The relative size of the carpal elements is: carpal

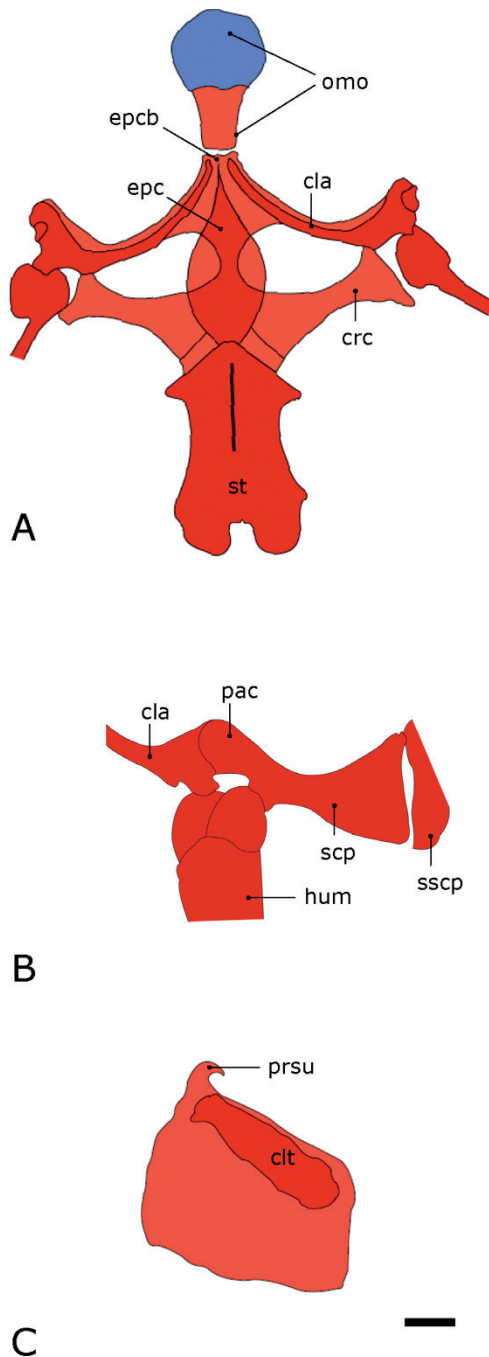


Figure 5. (A) Ventral and (B) lateral view of the pectoral girdle skeleton, (C) dorsal view suprascapula. Abbreviations: cla, clavicle; clt, cleithrum; crc, coracoid; epc, epicoracoid; epcb, epicoracoid bridge; hum, humerus; omo, omovertebral bone; pac, pars acromialis; prsu, suprascapular process; scp, scapula; sscp, suprascapula. Scale 1mm; blue: cartilage, red: mineralized bone; epc, crc depicted partly “semintransparent” to demonstrate the outline of both elements.

5-4-3 > ulnare > radiale > element Y > carpal 2 > proximal prepollex. The distal carpal 5-4-3 is articulated with all carpal elements, except the proximal prepollex, and it is articulated also to the proximal head of the metacarpals III, IV, and V. The prepollex has two elements, the proximal element being shorter than the distal, claw-shaped one. Both are completely ossified. The relative lengths of the metacarpals are IV > III > V > II. The relative lengths of the digits are IV > V > III > II, and the phalangeal formula is 2-2-3-3. Small, flat, and slightly calcified intercalary elements are articulated between the overlapping ventral and distal end of the penultimate phalange, and the dorsal and proximal end of the ultimate phalange. The distal phalanges are bottle-shaped. The proximal and distal ends, except those of the ultimate phalanges, are covered by calcified and fibrous tissue. No sesamoid elements were observed.

The elements of the pelvic girdle (Fig. 7) are ossified, except the slightly cartilaginous medial symphysis between each pubis. The ilia do not have ilial crests. Posteriorly, the ilia have a dorsal protuberance (=ilial protuberance sensu Maglia et al., 2007). The internal margins of the ilia are V-shaped in dorsal view. Medially the three elements are fused. The ischia are fused with the pubes. The anterior end is articulated with the lateroventral surface of the corresponding sacral diapophysis. The articulation

Figure 5. (A) Ventral and (B) lateral view of the pectoral girdle skeleton, (C) dorsal view suprascapula. Abbreviations: cla, clavicle; clt, cleithrum; crc, coracoid; epc, epicoracoid; epcb, epicoracoid bridge; hum, humerus; omo, omovertebral bone; pac, pars acromialis; prsu, suprascapular process; scp, scapula; sscp, suprascapula. Scale 1mm; blue: cartilage, red: mineralized bone; epc, crc depicted partly “semintransparent” to demonstrate the outline of both elements.

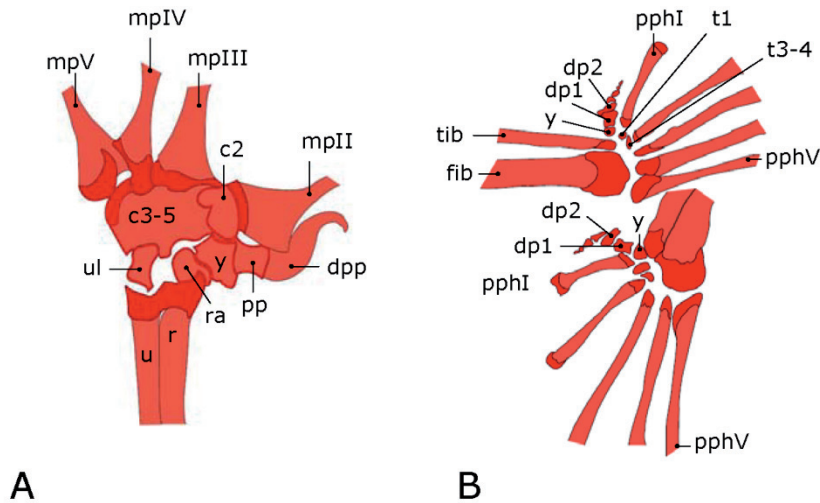


Figure 6. (A) Right hand in dorsal view, (B) left foot in dorsal (top) and ventral (bottom) view, not to scale. Abbreviations: c, carpals; dpp, distal prepollex; dp1, distal prehallux 1; dp2, distal prehallux 2; fib, fibulare; mp, manual phalanges; pp, prepollex; pph, pedal phalanges, r, radius; ra, radiale; t, tarsals; tib, tibiale; u, ulna; ul, ulnare; y, element Y.

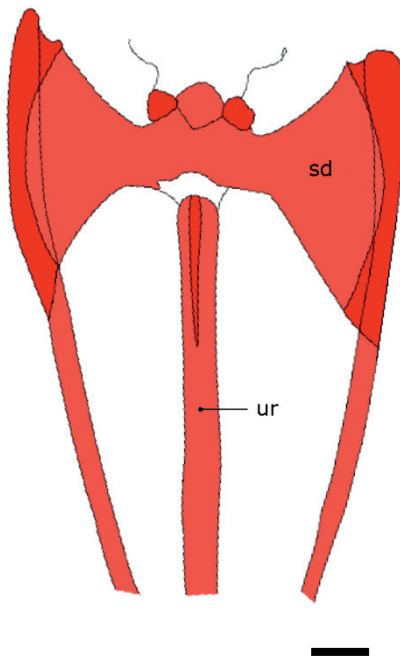


Figure 7. Pelvic skeleton, abbreviations: sd, sacral diapophysis; ur, urostyle. Scale 1 mm.

extends over nearly one third of the length of the ilial shaft. The ischium bears an interischadic crest which is located posterodorsal to the acetabular area, well developed and posteriorly flattened. The demarcation between the ischia and the pubes, and the pubes and the ilia are clearly visible. Also the articulation between the ilia and the ischia is clearly differentiated. The articulation of the ilia and the sacral diapophyses is articulation type I (Emerson, 1979).

The femur of the hindlimb is well ossified; the ventral and the posterior borders have a femoral crest along the posterior to the proximal end. This crest runs along one-seventh of the length of the femur. Proximally, the femur is slightly curved anteriorly. The tibiofibula is approximately equal in length to the femur. It is compressed and narrowed at the midshaft; the distal and proximal ends are equal in size, with grooves just proximally and distally.

The tibiale and fibulare of the pes (Fig. 6B) are nearly equal in length, and are fused distally and proximally. They are almost two-thirds as long as the tibiofibula. The relative sizes of

the tarsal elements are: $Y > 3 = 4 > 2$. The fibulare articulates directly with metatarsals III, IV, and V. The tarsal 2 articulates with the metatarsal I, and the tarsal 3-4 articulates with the metatarsals II and III. The element Y is ventral to the tarsal 1, and is articulated to the tibiale. The prehallux has four elements: the prehallux and three distal prehallical elements. The prehallux is ossified; the three distal prehallical elements are calcified and smaller than the prehallux. Relative lengths of the metatarsals are: $IV > V > III > II > I$. The relative lengths of the digits are: $IV > III = V > II > I$. The phalangeal formula (from digit I to V) is 2-2-3-4-3. The intercalary elements are small, slightly calcified, between the ventral end of the penultimate phalange and the dorsal end of the distal phalange. The distal phalange is bottle-shaped. No sesamoid elements could be demonstrated.

Larval osteology

The skeletal morphology of juvenile individuals is representatively described taking into account several cleared and stained specimens. The onset of ossification of the individual skeletal elements is shown in Fig. 8.

Cranium

In individuals at GS39/40 (Fig. 9), the cartilago labialis superior (sensu Haas, 1999); suprarostril cartilage (sensu Maglia and Púgener, 1998) of the chondrocranium is a discontinuous plate divided in a central corpus (corpus rostrale) and a posterior and dorso-laterally expanded ala (pars alaris Haas, 1999); the two parts are articulated. The suprarostril cartilages lack foramina but bear both notches on their ventral margins and small posterior processes. Every ala is posteriorly enlarged, and is dorsolateral and ventrally expanded. They are not fused but articulated to the cornu trabeculae. Each ala has three processes, two of which are articulated to the cornu trabeculae and one with the corpores suprarostrales. The dorsal posterior process (processus dorsalis) extends dorsad to the cartilage of Meckel. There are no fenestrations between corpus and ala. An adrostral cartilage is absent. The admandibular cartilages are present on the anteroventral margin of Meckel's cartilage. Meckel's cartilages are L-shaped structures, each projecting anteromedially and slightly dorsally to articulate with the infrarostral cartilage. Their proximal ends are articulated with the partes alares and with the corpus suprarostralis. The angle of divergence is nearly 25° . The cornua trabeculae form the planum ethmoidale; they are relatively short (one fifth of the length of the chondrocranium), taking into account a subterminal mouth, with a process for the joint of the ligamentum quadratoethmoidale. At the anterior end they support the suprarostril cartilages, and articulate laterally with the partes alares. Ventrally they are joined at the ethmoidal plate. The ethmoidal plate is formed at the posterior end of the cornua trabeculae. There is an association between the tectum nasi and the commissura quadratocranialis. The tectum nasi is formed by cartilage posterior to the choanae, dorsal to the ethmoidal plate. The basis cranii (basal plate) forms the floor of the braincase. It has neither a basicranial fenestra nor craniopalatal foramina. The otic capsules are ventrally perforated by a big fenestra ovalis, which is obscured by the cartilaginous operculum. The posterolateral border of the basis cranii shows a posterior process anterior to the otic capsule. The palatoquadrate is not articulated with the anterior part of the basis cranii with its great ala. There are three connections to the neu-

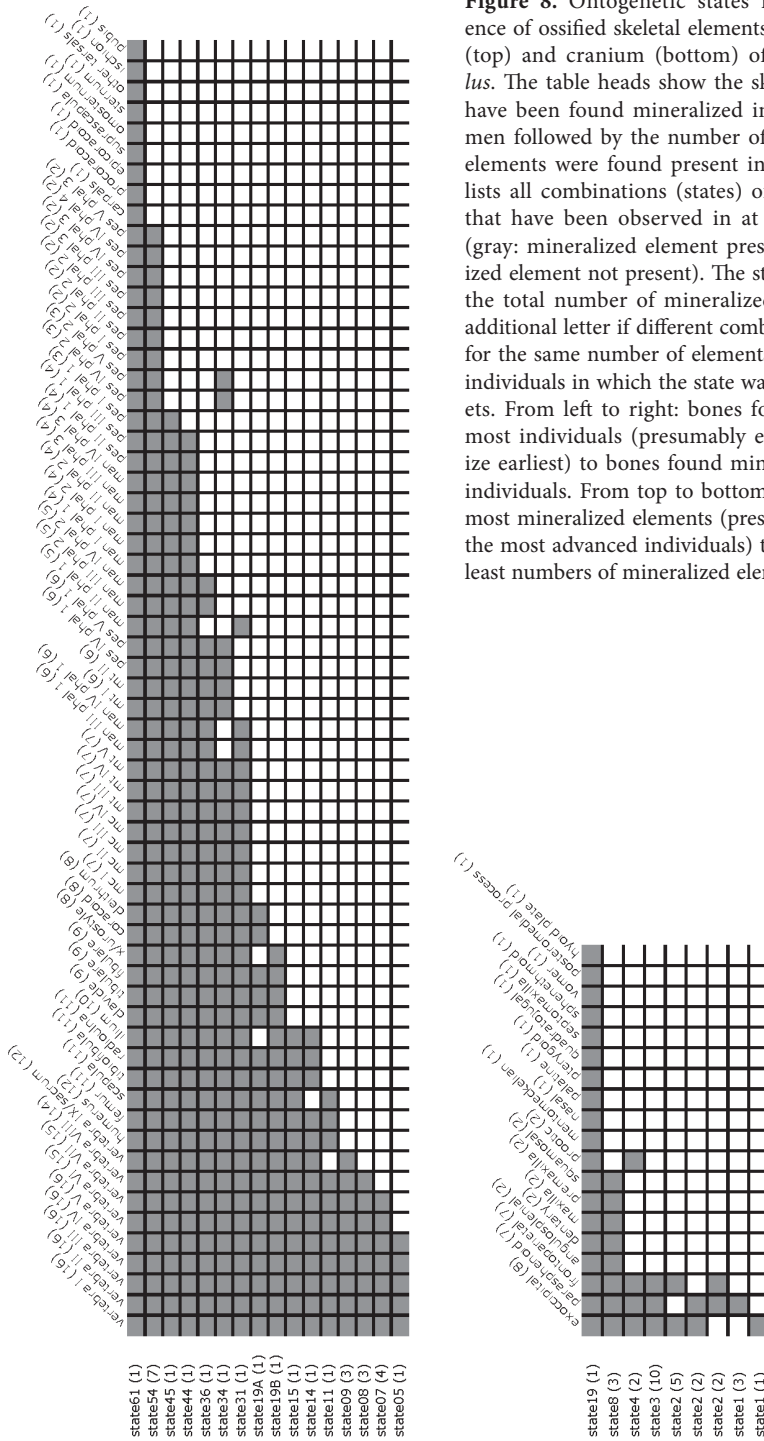


Figure 8. Ontogenetic states regarding the presence of ossified skeletal elements in the postcranium (top) and cranium (bottom) of *Hypsiboas pulchellus*. The table heads show the skeletal elements that have been found mineralized in at least one specimen followed by the number of states in which the elements were found present in brackets. The table lists all combinations (states) of mineralized bones that have been observed in at least one specimen (gray: mineralized element present, white: mineralized element not present). The states are named with the total number of mineralized elements, with an additional letter if different combinations were found for the same number of elements and the number of individuals in which the state was observed in brackets. From left to right: bones found mineralized in most individuals (presumably elements to mineralize earliest) to bones found mineralized in the least individuals. From top to bottom: states showing the most mineralized elements (presumably exhibited by the most advanced individuals) to states showing the least numbers of mineralized elements.

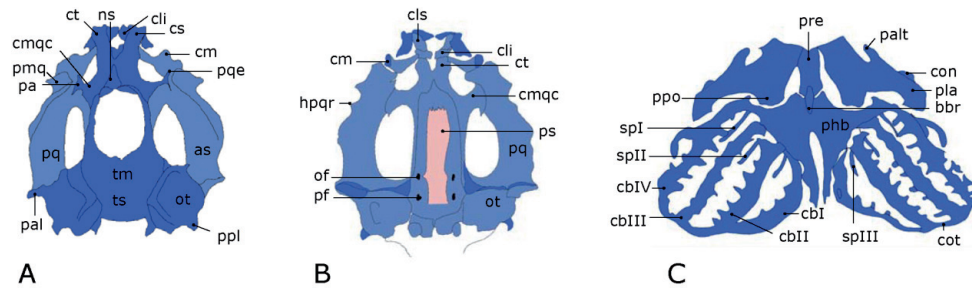


Figure 9. (A) Dorsal view and (B) ventral view of a tadpole (GS39-40) chondrocranium, (C) hyobranchial apparatus of a tadpole (GS39-40). Abbreviations: as, arcus subocularis; bbr, basibranchial; cb, ceratobranchials; cli, cartilago labialis inferior; cls, cartilago labialis superior; cm, Meckel's cartilage; cmqc, commissura quadratocranialis; cs, corpus suprarostralis; ct, cornu trabeculae; con, condylus articularis; hpqr, hyoquadrate processus; ns, nasal septum; of, optical foramen; ot, otic capsule; pa, processus antorbitalis; pal, processus anterolateralis; palt, processus anterolateralis; pf, prootic foramen; phb, planum hypobranchiale; pla, processus lateralis of certatobranchial; pmq, processus muscularis quadrati; ppl, processus posterolateralis; ppo, processus posterioris of ceratohyal; pq, palatoquadrate; pqe, processus quadratoetmoidalis; pre, pars reunion; ps, parasphenoid; sp, spiculae; tm, taenia tecti medialis; ts, tectum synoticum. Scale 1mm; blue: cartilage, red: mineralized bone.

rocranium: the commissura quadratocranialis anterior, the processus ascendens, and the otic connection. It is articulated to the commissura quadratocranialis anterior. This part of the palatoquadrate is the processus muscularis quadrati; the lateral side of the palatoquadrate forms the arcus subocularis. Ventral to the processus muscularis quadrati, the hyoquadrate process is located. The posterior end is articulated to the pila antotica by the ascending process of the palatoquadrate. The latter articulates with the pila antotica and with the ventral process of the tectum synoticum, anterior to the otic capsule. The processus muscularis quadrati is articulated to the commissura quadratocranialis. The palatoquadrate curvature and the processus anterolateralis of the crista parotica are in contact. At this stage, both the processus anterolateralis and the posterolateralis are elongated. The cartilaginous hyobranchial skeleton bears the copula I and II (sensu Maglia and Púgener, 1998; Sheil and Alamillo, 2005; basihyal and basibranchial respectively sensu Haas, 1999), the pars reuniens, the paired ceratohyalia, four pairs of ceratobranchials, and two hyobranchial plates (sensu Maglia and Púgener, 1998; Sheil and Alamillo, 2005; planum hypobranchiale sensu Haas, 1999). The ceratohyalia are the biggest cartilages in the hyobranchial apparatus. Each ceratohyal possesses an anterior process (=processus anterior sensu Haas, 1999), and a well-developed anterolateral process (=processus anterolateralis sensu Haas, 1999; hyoquadrate process sensu Maglia et al., 1998). This process is longer than the processus anterioris. The processus lateralis points posterolaterally. The large posterior process (=processus posterior sensu Haas, 1999) is nearly in central contact with the hypobranchial plate (=planum hypobranchiale sensu Haas, 1999). The pars reuniens is poorly chondrified, interconnects the ceratohyalia (=ceratohyals), and is articulated with the hypobranchial plates posteriorly. The hypobranchial plates are triangular, and articulate with each other along the medial margins; posterolaterally they articulate with the ceratobranchials, but are continuous with ceratobranchial I. The ceratobranchialia articu-

late distally via the commissurae terminalis. The width of the ceratobranchials is irregular; the ceratobranchials III and IV are the widest, whereas ceratobranchials I and II are the thinnest. Both ceratobranchials and each hypobranchial plate bear spiculae. Those in the hypobranchial plate are located at the end of the fusion of the hypobranchial with the ceratobranchial I.

Postcranium

In the youngest specimen investigated (GS 25), no postcranial skeletal elements could be found. At GS 28-31, in the axial skeleton, cartilaginous primordia of vertebral centra were present, anteriorly more advanced in development than posterior. Small rib primordia laterally to the neural arches of vertebrae II and III were present at GS 33 specimens, in which also sacral and postsacral vertebrae had begun to develop. At GS 34, transverse processes of vertebrae II to IV were present, although less pronounced in vertebra IV. Ventral ossifications in vertebrae I-IV could be observed in GS 36 specimens (hypoapophyses); a cartilaginous primordium of the urostyle (or the postsacral vertebra) was also present at this stage. Ossifications in the neural arches were found at GS 37, with the dorsal processes still cartilaginous, at the same time the transverse processes of vertebrae II-V were present. A cartilaginous primordium of the sacral diapophysis was developed at GS 39-40. An ossified hypochord and ossifications in postsacral vertebrae were not found before GS 41. At GS 42, at least primordial of transverse processes could be found up to vertebrae VIII, postsacral vertebrae were ossified by then. Vertebrae became discernible as procoelic.

Chondral primordia of the forelimb elements humerus, radius, radiale, and ulnare were present at GS 34; the anterior radiale (=r' sensu Fabrezi, 1993), carpals 5-4, and metacarpals IV-V could be found at GS 35. At GS 36, radiale (r' and r) and the primordium of the proximal phalanges of finger IV and V were present. At GS 37, when the longbones humerus, radius, and ulna had begun to ossify in the centers and at their ends, the cartilaginous carpals 5-4-3 and 2 and the proximal element of the prepollex were visible, the phalangeal formula of the hand was 1-2-3-3. Element Y (sensu Fabrezi, 1993) was found at GS 39/40. At GS 42, radius and ulna were nearly totally fused and the phalangeal formula was as in adults.

The cartilaginous hindlimb elements femur, tibia, fibula, tibiale, and fibulare were present at GS 34, at GS 35 metatarsals III, IV, and V were also found, at GS 36 the phalangeal formula was 1-1-1-2-2 and element Y was visible. At GS 37, at the beginning of the ossification of several longbones, the distal tarsals 1, 2, and 3 (or 2-3) and all metatarsals were discernible, and the phalangeal formula was 1-1-2-3-2.

The three elements of the pelvic girdle developed at GS 34; at the same stage the shoulder girdle was composed by cartilaginous procoracoids, coracoids, scapulae, and suprascapulae. At GS 37 a weakly developed epicoracoid was present and the scapula began to ossify. Clavicle and cleithrum could only be found from GS 42 onward.

DISCUSSION

In this study, we described the osteology and aspects of skeletal development of the hyloid frog *Hypsiboas pulchellus*. Regarding adult osteology, in *Hypsiboas pulchellus*, the

one aspect to highlight is the presence of a process in the suprascapula (herein processus suprascapularis) (Fig. 5C). This structure has not been demonstrated in any other anuran species to exhibit this specific shape. Maglia et al. (2007) described a similar process in a hylid, *Acris crepitans*. However, this process is morphologically different because it exhibits a more triangular shape (“anteriorly-projecting triangular process”, Maglia et al., 2007: 212).

Regarding skeletal development, general patterns reported previously for anuran and hylid skeletogenesis can be confirmed for *H. pulchellus*. Banbury and Maglia (2006) divided cranial development into five phases: 1) postembryonic (GS 30-33), 2) premetamorphic (GS 34-39), 3) early metamorphic (GS 39-42), 4) late metamorphic (GS 42-45), and 5) postmetamorphic. Following this schema in studying the relative timing of the onset of ossification (ossification sequence), the postembryonic stages comprise the onset of the ossification of the parasphenoid, presacral vertebrae I-VII, frontoparietal and exoccipital. During the premetamorphic phase, the onset of the ossification of the transverse processes of presacral vertebrae I-VIII, sacral vertebra IX, humerus, radioulna, ilium, femur, tibiofibula, and scapula occurs. In the early metamorphic phase the cleithrum, clavicle, coracoids, metacarpals, tarsals, metatarsals, phalanges, hypochord, and prootic begin to ossify. In the late metamorphic phase the angular, dentary, maxilla, premaxilla and squamosal ossify. In the postmetamorphic phase the sequence of ossification ends, remaining as such in adults.

To assess intraspecific/individual variability in the relative orders of onset of ossification in individual skeletal elements (ossification sequences), ideally in vivo observations would be necessary. Since however, the absolute number of ossified elements can be used as a measure of the developmental progress – transient elements removed – ossification sequences are in contrast to temporal orders of other developmental character sets relatively easy to reconstruct from preserved specimens without additional age information. We found intraspecific variation in both cranial and postcranial ossification sequences. Cranially, with one exception (the missing prootic in cranial state 08, Fig. 8), changes in order took place between elements that were temporally neighbored within ossification sequences, within this sample between exoccipital, parasphenoid, and frontoparietal. These elements have been reported to be among the first cranial elements to ossify in a variety of anurans (Hanken and Hall, 1988; Wiens, 1989; Dunlap and Sanchiz, 1996; Púgener and Maglia, 1997; Haas, 1999; Wild, 1999; Trueb et al. 2000; Banbury and Maglia, 2006). Within anurans, changes in the relative order of ossification of these elements have been reported before for the tailed frog, *Ascaphus truei* (Moore and Townsend jr., 2003), and are evident for the hyperossified frog, *Pyxicephalus adspersus* (Haas, 1999; Sheil, 1999). In the postcranium, elements found involved in changes in the sequence of ossification were the sacrum, scapula, ilium, urostyle, and phalanges of hands and feet; the variability in relative onset time of ossification in the latter had previously been reported for a number of other tetrapod taxa including birds, turtles, and mammals (Rieppel, 1993; Sheil and Greenbaum, 2005; Maxwell, 2008; Sánchez-Villagra et al., 2009; Wilson et al., 2010; Mitgutsch et al., 2011). Intraspecific variability, as known from osteological and other morphological data, should thus also for ossification sequences be carefully accounted for in comparative studies. Research on a variety of aspects regarding the intraspecific variation found in ossification sequences such as temporal distribution or taxonomic differences will be additional important steps in understanding the evolution of skeletal development.

ACKNOWLEDGEMENTS

We thank the Pontificia Universidad Javeriana (JMH) and the Paläontologisches Institut und Museum, Universität Zürich, Zürich, Switzerland for support. We also thank Catalina Mantilla for preparing the final drawings and two anonymous reviewers for helpful comments on an earlier version of this manuscript.

REFERENCES

- Báez, A.M. (2000): Tertiary Anura of South America. In: Amphibian Biology, V. 4: Palaeontology, p. 1388–1401. Heatwole, H., Carroll, R.L. Eds, Chipping Norton: Surrey Beatty & Sons.
- Balanoff, A.M., Rowe, T. (2007): Osteological description of an embryonic skeleton of the extinct elephant bird, *Aepyornis* (Palaeognathae: Ratitae). *J. Vert. Paleontol.* **27** (suppl.): 1–53.
- Banbury, B., Maglia A.M. (2006): Skeletal development of the Mexican spadefoot, *Spea multiplicata* (Anura: Pelobatidae). *J. Morphol.* **267**: 803–821.
- Bininda-Emonds, O.R.P., Jeffrey J.E., Richardson M.K. (2003): Is sequence heterochrony an important evolutionary mechanism in mammals? *J. Mammal. Evol.* **10**: 335–361.
- Callery, E.M. (2006): There is more than one frog in the pond: a survey of the Amphibia and their contributions to developmental biology. *Seminars Cell. Dev. Biol.* **17**: 80–92.
- Clarke, B.T. (2007): Comparative morphology and amphibian taxonomy: an example from the osteology of discoglossoid frogs. In: Amphibian Biology. V. 7: Systematics, p. 2465–2612. Heatwole, H., Tyler, M.J., Eds, Chipping Norton: Surrey Beatty & Sons.
- Crump, M.L. (2009): Amphibian diversity and life history In: Amphibian Ecology and Conservation. A Handbook of Techniques, p.3–20. Dodd, C. K., Ed, Oxford University Press, USA.
- de Sá, R.O. (1988): Chondrocranium and ossification sequence of *Hyla lanciformis*. *J. Morphol.* **195**: 345–355.
- de Sá, R.O., Hill, S. (1998): Chondrocranial anatomy and skeletogenesis in *Dendrobates auratus*. *J. Herpetol.* **32**: 205–210.
- de Sá, R.O., Trueb, L. (1991): Osteology, skeletal development, and chondrocranial structure of *Hamptophryne boliviana* (Anura: Microhylidae). *J. Morphol.* **209**: 311–330.
- Dingerkus, G., Uhler L.D. (1977): Enzyme clearing of alcian blue stained whole small vertebrates for demonstration of cartilage. *Stain Tech.* **52**: 229–232.
- Duellman, W.E., Trueb, L. (1994): *Biology of Amphibians* Baltimore: The Johns Hopkins University Press. USA.
- Dunlap, K.D., Sanchiz, B. (1996): Temporal dissociation between the development of the cranial and appendicular skeletons in *Bufo bufo* (Amphibia: Bufonidae). *J. Herpetol.* **30**: 506–513.
- Emerson, S.B. (1979): The ilio-sacral articulation in frogs: form and function. *Biol. J. Linn. Soc.* **11**: 153–168.
- Fabrezi, M. (1993): The anuran tarsus. *Alytes* **11**: 47–63.

- Gaudin, A.J. (1973): The development of the skull in the Pacific tree frog, *Hyla regilla*. *Herpetologica* **29**: 205-218.
- Gaupp, E. (1896) A. Ecker's und R. Wiedersheim's Anatomie des Frosches. Friedrich Vieweg und Sohn, Braunschweig.
- Germain, D., Laurin, M. (2009): Evolution of ossification sequences in salamanders and urodele origins assessed through event-pairing and new methods. *Evol. Dev.* **11**: 170-190.
- Gosner, K.L. (1960): A simplified table for staging anuran embryos and larvae with notes on identification. *Herpetologica* **16**: 83-190.
- Gurdon J.B., Hopwood, N. (2000): The introduction of *Xenopus laevis* into developmental biology: of empire, pregnancy testing and ribosomal genes. *Int. J. Dev. Biol.* **44**: 43-50.
- Haas, A. (1995): Cranial features of dendrobatid larvae (Amphibia: Anura: Dendrobatidae). *J. Morphol.* **224**: 241-264.
- Haas, A. (1996): Das larvale Cranium von *Gastrotheca riobambae* und seine Metamorphose (Amphibia, Anura, Hylidae). *Verh. Naturwiss. Ver. Ham.* **36**: 33-162.
- Haas, A. (1999): Larval and metamorphic skeletal development in the fast-developing frog *Pyxicephalus adspersus* (Anura, Ranidae). *Zoomorphology* **119**: 23-35.
- Hanken, J., Hall, B.K. (1984): Variation and timing of the cranial ossification sequence of the oriental fire-bellied toad, *Bombina orientalis* (Amphibia, Discoglossidae). *J. Morphol.* **182**: 245-255.
- Hanken, J., Hall, B.K. (1988): Skull development during anuran metamorphosis. I. Early development of the first three bones to form – the exoccipital, the parasphenoid, and the frontoparietal. *J. Morphol.* **195**: 247-256.
- Hanken, J., Klymkowsky, W., Summers, C.F., Seufert, W., Ingebrigtsen, N. (1992): Cranial ontogeny in the direct-developing frog, *Eleutherodactylus coqui* (Anura: Leptodactylidae), analyzed using whole-mount immunohistochemistry. *J. Morphol.* **211**: 95-118.
- Harrison, L.B., Larsson, H.C.E. (2008): Estimating evolution of temporal sequence changes: a practical approach to inferring ancestral developmental sequences and sequence heterochrony. *Syst. Biol.* **57**: 378-387.
- Jeffery, J.E., Bininda-Emonds, O.R.P., Coates, M.I., Richardson, M.K. (2002a): Analyzing evolutionary patterns in amniote embryonic development. *Evol. Dev.* **4**: 292-302.
- Jeffery, J.E., Richardson, M.K., Coates, M.I., Bininda-Emonds, O.R.P. (2002b): Analyzing developmental sequences within a phylogenetic framework. *Syst. Biol.* **51**: 478-491.
- Jeffery, J.E., Bininda-Emonds, O.R.P., Coates, M.I., Richardson, M.K. (2005): A new technique for identifying sequence heterochrony. *Syst. Biol.* **54**: 230-240.
- Kerney, R., Gross, J.B., Hanken, J. (2010): Early cranial patterning in the direct-developing frog *Eleutherodactylus coqui* revealed through gene expression. *Evol. Dev.* **12**: 373-382.
- Kerney, R., Meegaskumbura, M., Manamendra-Arachchi, K., Hanken, J. (2007): Cranial ontogeny in *Philautus silus* (Anura: Ranidae: Rhacophorinae) reveals few similarities with other direct-developing anurans. *J. Morphol.* **268**: 715-725.
- Koenemann, S., Schram, F.R. (2002): The limitations of ontogenetic data in phylogenetic analyses. *Contrib. Zool.* **71**: 47-65.

- Larson, P.M., de Sá, R.O. (1998): Chondrocranial morphology of *Leptodactylus* larvae (Leptodactylidae: Leptodactylinae): its utility in phylogenetic reconstruction. *J. Morphol.* **238**: 287–305.
- Larson, P.M. (2002): Chondrocranial development in larval *Rana sylvatica* (Anura: Ranidae): morphometric analysis of cranial allometry and ontogenetic shape change. *J. Morphol.* **252**: 131–144.
- Larson, P.M., de Sá, R.O., Arrieta, D. (2003): Chondrocranial, hyobranchial and internal oral morphology in larvae of the basal bufonid genus *Melanophryniscus* (Amphibia: Anura). *Acta Zool.* **154**: 145–154.
- Lynch, J.D. (1971): Evolutionary relationships, osteology, and zoogeography of leptodactylid frogs. *Misc. Pub. Mus. Nat. Hist. Univ. Kansas* **53**: 1–238.
- Mabee, P.M., Olmstead, K.L., Cubbage, C.C. (2000): An experimental study of intraspecific variation, developmental timing, and heterochrony in fishes. *Evolution* **54**: 2091–2106.
- Mabee, P.M., Trendler, T.A. (1996): Development of the cranium and paired fins in *Betta splendens* (Teleostei: Percomorpha): intraspecific variation and interspecific comparisons. *J. Morphol.* **227**: 249–287.
- Maglia, A.M., Púgener, L.A. (1998): Skeletal development and adult osteology of *Bombina orientalis* (Anura: Bombinatoridae). *Herpetologica* **54**: 344–363.
- Maglia, A.M., Púgener, L.A., Mueller, J.M. (2007): Skeletal morphology and postmetamorphic ontogeny of *Acris crepitans* (Anura: Hylidae): a case of miniaturization in frogs. *J. Morphol.* **268**: 194–223.
- Maxwell, E.E. (2008): Ossification sequence of the avian order Anseriformes, with comparison to other precocial birds. *J. Morphol.* **269**: 1095–1113.
- Mitgutsch, C., Wimmer, C., Sánchez-Villagra, M.R., Hahnloser, R., Schneider, R.A. (2011): Timing of ossification in duck, quail, and zebra finch: intraspecific variation, heterochronies, and life history evolution. *Zool. Sci.* **28**: 491–500.
- Moore, M.K., Townsend jr., V.R. (2003): Intraspecific variation in cranial ossification in the tailed frog, *Ascaphus truei*. *J. Herpetol.* **37**: 714–717.
- Nunn, C.L., Smith, K.K. (1998): Statistical analyses of developmental sequences: the craniofacial region in marsupial and placental mammals. *Am. Nat.* **152**: 82–101.
- Poe, S., Wake, M.H. (2004): Quantitative tests of general models for the evolution of development. *Am. Nat.* **164**: 415–422.
- Púgener, L.A., Maglia, A.M. (1997): Osteology and skeletal development of *Discoglossus sardus* (Anura: Discoglossidae). *J. Morphol.* **233**: 267–286.
- Rage, J.C., Roček, Z. (2000): Tertiary Anura of Africa, Asia, Europe and North America. In *Amphibian Biology*. V. 4: Palaeontology, p. 1332–1387. Heatwole, H., Carroll, R.L., Eds, Chipping Norton: Surrey Beatty & Sons.
- Ramaswami, L.S. (1944): The chondrocranium of two torrent-dwelling anuran tadpoles. *J. Morphol.* **74**: 347–374.
- Richardson, M.K., Jeffery, J.E., Coates, M.I., Bininda-Emonds, O.R.P. (2001): Comparative methods in developmental biology. *Zoology* **104**: 278–283.
- Rieppel, O. (1993): Studies on the skeleton formation in reptiles: patterns of ossification in the skeleton of *Chelydra serpentina* (Reptilia, Testudines). *J. Zool.* **231**: 487–509.
- Rose, C.O., Reiss, J.O. (1993): Metamorphosis and the vertebrate skull: ontogenetic patterns and developmental mechanisms. In: *The Skull*. Volume 1: Development, p.

- 289–346. Hanken, J., Hall, B.K., Eds, The University of Chicago Press, Chicago - London.
- Roček, Z. (2000): Mesozoic anurans. In: Amphibian Biology. V. 4: Palaeontology, p. 1295–1331. Heatwole, H., Carroll, R.L., Eds, Chipping Norton: Surrey Beatty & Sons.
- Roček, Z. (2003): Larval development and evolutionary origin of the anuran skull. In: Amphibian Biology. V. 5: Osteology, p. 1877–1995. Heatwole, H., Davies, M., Eds, Chipping Norton: Surrey Beatty & Sons.
- Sánchez-Villagra, M.R., Müller, H., Sheil, C.A., Scheyer, T.M., Nagashima, H., Kuratani, S. (2009): Skeletal development in the Chinese soft-shelled turtle *Pelodiscus sinensis* (Testudines: Trionychidae). *J. Morphol.* **270**: 1381–1399.
- Schulmeister, S., Wheeler, W. C. (2004): Comparative and phylogenetic analysis of developmental sequences. *Evol. Dev.* **6**: 50–57.
- Sheil, C.A. (1999): Osteology and skeletal development of *Pyxicephalus adspersus* (Anura: Ranidae: Raninae). *J. Morphol.* **240**: 49–75.
- Sheil, C.A., Alamillo, H. (2005): Osteology and skeletal development of *Phyllomedusa vailanti* (Anura: Hylidae: Phyllomedusinae) and a comparison of this arboreal species with a terrestrial member. *J. Morphol.* **265**: 343–368.
- Sheil, C.A., Greenbaum, E. (2005): Reconsideration of skeletal development of *Chelydra serpentina* (Reptilia: Testudinata: Chelydridae): evidence for intraspecific variation. *J. Zool.* **265**: 235–267.
- Stöhr, P. (1881) Zur Entwicklungsgeschichte des Anurenschädels. *Z. wiss. Zool.* **36**: 68–103.
- Stokely, P.S., List, J.C. (1954): The progress of ossification in the skull of the cricketfrog *Pseudacris nigrata triseriata*. *Copeia* **1954**: 211–217.
- Swart, C., de Sá, R.O. (1999): The chondrocranium of the Mexican Burrowing Toad, *Rhinophrynus dorsalis*. *J. Herpetol.* **33**: 23–28.
- Trueb, L. (1970): Evolutionary relationships of casque-headed tree frogs with co-ossified skulls (family Hylidae). *Univ. Kansas Publ. Mus. Nat. Hist.* **18**: 547–716.
- Trueb, L. (1973): Bones, frogs, and evolution. In: *Evolutionary Biology of the Anurans. Contemporary Research on Major Problems*, p.65–132. Vial, J.L., Ed, Columbia: University of Missouri Press.
- Trueb, L. (1993): Patterns of cranial diversity among the Lissamphibia. In: *The Skull. V.2: Patterns of Structural and Systematic Diversity*, p. 255–343. Hanken, J., Hall, B.K., Eds, Chicago - London: The University of Chicago Press.
- Trueb, L., Alberch, P. (1985): Miniaturization and the anuran skull: a case study of heterochrony. *Fortschr. Zool.* **30**: 113–121.
- Trueb, L., Pügener, L.A., Maglia, A.M. (2000): Ontogeny of the bizarre: an osteological description of *Pipa pipa* (Anura: Pipidae), with an account of skeletal development in the species. *J. Morphol.* **243**: 75–104.
- Trueb, L., Báez, A.M. (2006). Revision of the Early Cretaceous *Cordicephalus* from Israel and an assessment of its relationships among pipoid frogs. *J. Vert. Pal.* **26**: 44–59.
- van Eeden, J.A. (1951): The development of the chondrocranium of *Ascaphus truei* Stejneger with special reference to the relations of the palatoquadrate to the neurocranium. *Acta Zool.* **32**: 41–176.
- Vogt, C. (1842): Untersuchungen über die Entwicklungsgeschichte der Geburtshelferkroete (*Alytes obstetricans*). Solothurn: Verlag von Jent und Gassmann.

- Weisbecker, V., Goswami A., Wroe, S., Sánchez-Villagra, M.R. (2008): Ossification heterochrony in the therian postcranial skeleton and the marsupial-placental dichotomy. *Evolution* **62**: 2027-2041.
- Weisbecker, V., Mitgutsch, C. (2010): A large-scale survey of heterochrony in anuran cranial ossification patterns. *J. Zool. Syst. Evol. Res.* **48**: 332–347.
- Wiens, J.J. (1989): Ontogeny of the skeleton of *Spea bombifrons* (Anura: Pelobatidae). *J. Morphol.* **202**: 29–51.
- Wild, E.R. (1999): Description of the chondrocranium and osteogenesis of the Chacoan burrowing frog, *Chacophrys pierotti* (Anura: Leptodactylidae). *J. Morphol.* **242**: 229–246.
- Wilson, L.A.B., Schradin, C., Mitgutsch, C., Galliari, F.C., Mess, A., Sánchez-Villagra, M.R. (2010): Skeletogenesis and sequence heterochrony in rodent evolution, with particular emphasis on the African striped mouse (*Rhabdomys pumilio*). *Org. Div. Evol.* **10**: 243-258.
- Yeh, J. (2002): The evolution of development: two portraits of skull ossification in pipoid frogs. *Evolution* **56**: 2484–2498.